New Journal of Physics
An Institute of Physics and Deutsche Physikalische Gesellschaft Journal

Magnetic behaviour of thin films produced by depositing pre-formed Fe and Co nanoclusters

C Binns† and M J Maher

Department of Physics and Astronomy, University of Leicester, Leicester LE1 7RH, UK

New Journal of Physics **1** (2002) 1.1–1.15 (http://www.njp.org/)
Received 12 August 2002
Published

Abstract. We have studied the magnetic behaviour of ultra-thin films produced by depositing pre-formed gas phase Fe and Co nanoclusters, containing typically a few hundred atoms, in ultra-high vacuum (UHV) conditions. Two types of sample were prepared, that is, clusters embedded at very low volume fractions ($\leq 2\%$) within Ag matrices to obtain the isolated particle properties, and pure cluster-assembled films with no matrix that were transferred without a capping layer into the magnetometer in UHV. The dilute assemblies both display ideal superparamagnetism, with an H/T scaling of the magnetization curves, above 50 K for Fe clusters and 150 K for Co clusters. Fitting the magnetization data above these temperatures to Langevin functions enabled an accurate determination of the size distribution and gave a median size of 3 nm for the Fe and 2.8 nm for the Co clusters. At 2 K the magnetic isotherms are characteristic of assemblies of blocked particles with a uniaxial anisotropy axis and anisotropy constants of 2.6×10^5 and 7.7×10^5 J m^{-3} for Fe and Co particles respectively. The magnetic behaviour of the pure cluster films was analysed using a random anisotropy model including parameters determined from the isolated cluster films. The approach to saturation of the Fe and Co cluster films indicates that the ground state is a correlated super-spin glass over the temperature range 10–300 K in both cases.

1. Introduction

The behaviour of magnetic nanoparticles has fascinated materials scientists for decades [1]. Below a critical dimension of tens of nanometres the formation of magnetic domains becomes energetically unfavourable and the particles behave as giant moments of ferromagnetically

† Author to whom any correspondence should be addressed.

coupled atomic spins. These can be thermally excited across the particles' anisotropy barrier [2] in timescales varying from nanoseconds to aeons or the giant moment can form a superposition by quantum mechanical tunnelling through the barrier [3]–[5].

At $T = 0$ K, reversing the direction of the cluster magnetization requires an external field to drive the magnetization vector across the anisotropy boundary KV separating different magnetic alignments, where K is the anisotropy constant and V is the particle volume. At finite temperatures, the external field must also compete with thermal fluctuations of the moment. When a saturating field is removed from a particle (or a dilute assembly) at temperature T, the magnetization decays with a relaxation rate, τ, that can be approximated by the Arrhenius relationship:

$$\frac{1}{\tau} = f_0 \exp\left(\frac{-KV}{k_B T}\right), \tag{1}$$

where f_0 is the natural gyromagnetic frequency of the particle. For volumes typical in deposited gas-phase clusters, observations must be made at cryogenic temperatures ($\leq$5 K) for the magnetic relaxation to be slower than typical measurement times. At room temperature, the thermal energy $k_B T$ is much greater than the anisotropy energy of each particle so that all magnetization directions are almost energetically equal. The magnetization is then described by the classical Langevin function:

$$M = N\mu\left[\coth\left(\frac{\mu H}{k_B T}\right) - \frac{k_B T}{\mu H}\right], \tag{2}$$

where μ is the magnetic moment of each cluster. This can be several hundred atomic spins and so, unlike isolated atoms where very low temperatures or very high fields are required to achieve saturation, assemblies of clusters can be saturated easily. This state is referred to as superparamagnetism. The temperature at which half the cluster moments have relaxed during the time of a measurement is known as the blocking temperature, T_B, and only a narrow temperature region around T_B separates, essentially, permanently frozen moments from superparamagnetism.

The subject has received new impetus due to the development of cluster sources able to pre-form clusters in the gas phase, mass-select them and deposit them onto surfaces or embed them within matrices in ultra-high vacuum (UHV) conditions [6]. As free particles it is found by gradient field deflection measurements that, for diameters below about 2.4 nm ($\sim$600 atoms), Fe, Co and Ni particles show large enhancements of the total magnetic moment per atom relative to the bulk value [7, 8]. The particles retain an enhanced magnetization when they are deposited onto surfaces in UHV and x-ray magnetic circular dichroism (XMCD) measurements reveal that much of this enhancement comes from a substantial increase in orbital magnetism [9]–[13].

The same technology can be used to produce granular materials by co-depositing the clusters and a matrix material from a conventional MBE-type source onto a common substrate. The main advantages of this technique, not available in other production methods, are that it is possible to vary the size and volume fraction of the grains independently and to produce granular forms of miscible metal mixtures. These attributes have produced much interest in cluster deposition as a technique for producing high performance magnetic materials. Examples include high saturation moment films [29] and GMR sensors [15].

In all such industrial applications, the required cluster volume fraction is high—at or near the percolation threshold—so there are strong interactions between the clusters. In order to understand the behaviour of interacting cluster assemblies it is interesting to study the high

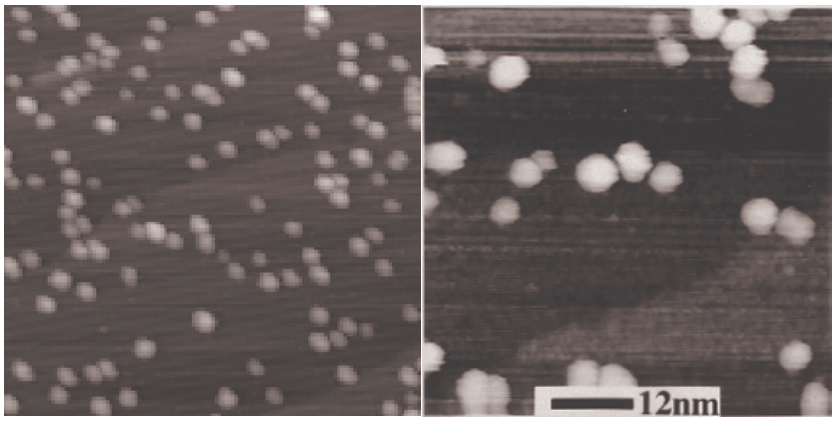

Figure 1. (a) STM image (100 nm × 100 nm) of un-filtered Fe clusters on Si(111). (b) A higher magnification (40 nm × 40 nm) image from the same film.

volume fraction limit, that is, pure magnetic cluster films deposited with no matrix. Previous studies have shown that above a critical cluster size, there is no liquid-like coalescence and the particles stack randomly on the surface though there may be sintering. The critical size for coalescence depends on the deposition conditions but for simple and noble metals is typically a few hundred atoms (2–3 nm) [16]–[19]. For transition metals it is much smaller and it can be safely assumed that the Fe and Co nanoclusters in this work, with sizes around 3 nm, stack randomly to form the film. Typical examples are shown in figure 1, which displays previously reported STM images of Fe clusters produced by our source deposited on Si(111) [20]. It is observed that the clusters do not coalesce but retain a distinct boundary, though the precise nature of the interfaces remains uncertain.

It is clear that the ground state magnetic configuration of a randomly stacked cluster film as in figure 1 will be different to one formed by depositing atoms. For example cluster films do not appear to form domains. To analyse the magnetic data we have used a random anisotropy (RA) model developed by several authors in the last two decades [21]–[24]. In the RA formalism, the magnetic ground state in a granular film is determined by the relative strength of an RA field:

$$H_r = \frac{2K_r}{M_s}, \tag{3}$$

and an exchange field:

$$H_{ex} = \frac{2A}{M_s R_a^2}, \tag{4}$$

where K_r is the (randomly oriented) anisotropy of the grains, M_s is their saturation magnetization, A is the exchange constant for the interaction between the grains and R_a is the nanometre sized region over which the local anisotropy axis is correlated, i.e. the characteristic grain size. Their relative strength is given by the dimensionless parameter

$$\lambda_r = \frac{H_r}{H_{ex}} = \frac{K_r {R_a}^2}{A}. \tag{5}$$

The model was developed to describe amorphous films in which a local, randomly oriented, anisotropy is due to local atomic order. It is even better suited to providing a description of

the magnetization in cluster-assembled films in which the distance R_a over which an anisotropy axis is correlated is well defined (i.e. the particle diameter). In addition, as pointed out by Loffler *et al* [26], the exchange interaction at the boundaries between particles is weaker than the intra-particle atomic exchange, further reinforcing the image of separate but interacting particles.

For $\lambda_r > 1$ the magnetic correlation length at zero field is R_a, and the magnetic vector in each particle points along the local intra-particle anisotropy axis. Note that in an arrow representation this state would be identical to that in isolated non-interacting particles at absolute zero. This regime is illustrated in figure 2(b). With increasing inter-particle exchange (or decreasing intra-particle anisotropy) the configuration becomes a correlated super-spin glass (CSSG) in which the magnetization vector in neighbouring particles is nearly aligned but the random deviation of the moments from perfect alignment produces a smooth rotation of the magnetization throughout the system with a magnetic correlation length that is a factor $1/\lambda_r^2$ larger than the particle diameter. This regime is illustrated in figure 2(c). The absolute value of λ_r marking the crossover between the two regimes depends on a number of factors including the angular distribution of the anisotropy axes, which may not be truly random. For example Loffler *et al* [26] showed that a cluster-assembled film in which $\lambda_r = 2$ was in the CSSG state. The disordered CSSG state is fragile and application of a small field produces a 'ferromagnet with wandering axes' (FWA) [22] with an approach to saturation that follows a $1/\sqrt{H}$ dependence in three dimensions [22] and a $1/H$ dependence in two dimensions [21]. These both change to a $1/H^2$ dependence above a crossover field [24] $H_{co} = 2A/M_s {R_a}^2$.

The RA model has been used previously to analyse magnetization data from cluster-assembled films [26]–[28] but here we apply it to cluster films that have been prepared without detectable contamination and transferred into a vibrating sample magnetometer (VSM) in UHV conditions. Thus we have been able to study exposed films without a protective non-magnetic capping layer. We have shown previously [29] that coatings used to protect films during transfer through air have a profound influence on the magnetic behaviour of the film.

The approach used in this work was to initially prepare and study dilute Fe and Co cluster films embedded in Ag at very low volume fractions (1–2%). The magnetization isotherms well above the cluster blocking temperature show perfect superparamagnetism and yield accurately the size distribution. Analysis of the curves below the blocking temperature gives the symmetry of the anisotropy and a good estimate of its magnitude. This information can then be fed into the RA model used to analyse the pure cluster films.

2. Film preparation and measurements

Fe and Co nanoclusters were formed using a UHV-compatible gas aggregation source described elsewhere [30]. The dilute films were prepared by co-depositing the clusters and Ag vapour from a conventional Knudsen cell evaporation source onto poly-ether–ether–ketone (PEEK) substrates of dimension $10\ \mathrm{mm} \times 10\ \mathrm{mm}$. Since the clusters were embedded these samples could be transferred into the magnetometer through air. The pure cluster films were deposited onto a PEEK rod that could be sealed *in situ* in a PEEK ampoule and transferred into the magnetometer without breaking vacuum. The system has been thoroughly tested and proven to maintain uncapped films without any detectable contamination [29]. A summary of the samples studied is shown in table 1. Magnetization isotherms were obtained using a VSM operating at fields of up to 9 T and temperatures down to 1.5 K.

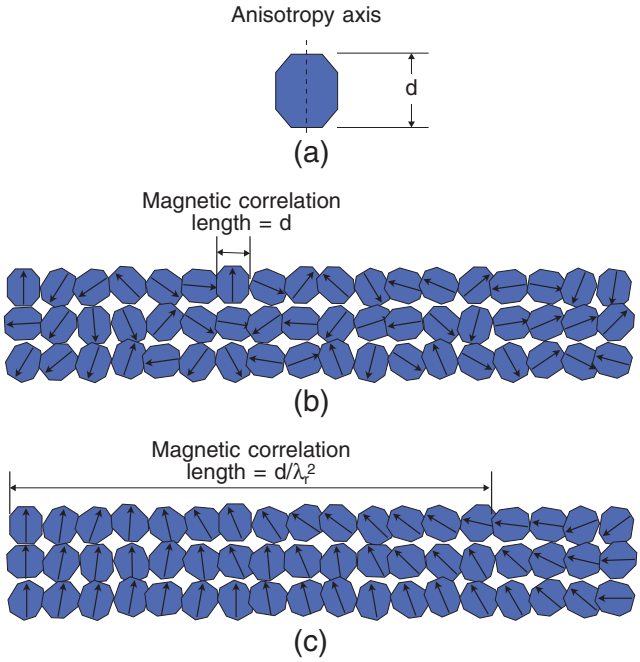

Figure 2. (a) Schematic representation of a magnetic nanoparticle with a uniaxial anisotropy axis (represented by a slight elongation); (b), (c) a stack of particles with randomly oriented anisotropy axes. In (b) $\lambda_r \geq 1$ and the magnetization vector points along the local anisotropy axis so the magnetic correlation length is a single particle diameter. In (c) $\lambda_r < 1$ and the magnetic vectors are nearly aligned. The random perturbation from perfect alignment results in a finite magnetic correlation length that is a factor $1/\lambda_r^2$ larger than a single particle.

Table 1. Samples reported in this study. All films contain Fe or Co clusters with a log-normal size distribution shown in figures 3 and 4.

Sample	Fe volume fraction (%)	Total film thickness (nm)	Capping layer	Median cluster diameter (nm)
S1 (Fe)	0.8 ± 0.2	850 ± 150	5 nm Ag	3.0
S2 (Co)	2 ± 0.4	720 ± 140	5 nm Ag	2.8
S3 (Fe)	100	5 ± 1	No cap	
S4 (Co)	100	20 ± 4	No cap	

3. Results and discussion

3.1. Dilute Fe cluster assemblies above the blocking temperature

Magnetic isotherms from sample S1 ($Fe_{0.8}Ag_{99.2}$) in the temperature range 50–300 K are shown in figure 3(a) (symbols). Each was fitted by a set of Langevin functions with different moment values where the amplitude of each Langevin function was a fitting variable. Ten size bins were used in the range 0.5–8 nm and the average amplitude as a function of particle size (moment)

after fitting all data sets is shown in the inset in figure 3(a). The calculated curves are displayed as lines and the fit is excellent in every case. The size distribution is the usual asymmetric shape and fitting it to a log-normal distribution (inset) gives a most probable cluster size of 2.57 nm with a standard deviation of 1.95 giving a median diameter of 3.0 nm. This distribution is similar to those obtained by direct STM imaging of deposited cluster films (e.g. figure 1). It was pointed out by Allia [31] however that this procedure is hazardous. In an interacting system it is possible to obtain an excellent Langevin fit with an 'apparent size' that is different to the real size and varies with temperature. We can therefore devise three tests to demonstrate ideal superparamagnetism with no interactions in this sample.

- The isotherms should display no hysteresis.
- The isotherms should scale with H/T.
- The fitted size distribution should be independent of temperature.

The lack of hysteresis is evident and the other two conditions are demonstrated in figure 3(b), which is the data in figure 3(a) re-plotted against H/T and an inset that shows the invariance with temperature of the median size obtained from the Langevin fits. This sample thus displays perfect superparamagnetism above 50 K.

3.2. Dilute Co cluster assemblies above the blocking temperature

The magnetic isotherms for sample S2 (Co_2Ag_{98}) in the temperature range 50–300 K are shown in figure 4(a) (symbols) along with the Langevin fits using the procedure described above (curves). In this case the fitted median size displayed in the inset in figure 4(b) is temperature dependent below about 150 K. This could either be due to weak dipolar interactions at the slightly higher volume fraction [31] or to the much higher anisotropy of the Co clusters relative to Fe (see below) requiring a higher temperature to reach the superparamagnetic limit. In either case the superparamagnetic limit is reached at a temperature ~ 150 K. This is also demonstrated in figure 4(b) in which the same data are plotted against H/T and only the 100 and 50 K curves are visibly seperated from the rest. Thus we can obtain the size distribution by Langevin fits as described above to the curves taken at 150 K and above. The result along with the fitted log-normal distribution is shown in the inset in figure 4(a) and for the Co clusters the most probable size is 2.45 nm with a standard deviation of 1.81 giving a median diameter of 2.8 nm.

3.3. Dilute Fe cluster assemblies below the blocking temperature

At 2 K most of the clusters in sample S1 ($Fe_{0.8}Ag_{99.2}$) are below the blocking temperature and as shown in figure 5(a) the magnetic isotherm develops hysteresis. The remanence, M_r, of an assembly of blocked particles reveals the symmetry of the anisotropy axes and their distribution in space. For example uniaxial anistropy axes randomly distributed over three dimensions give $M_r/M_s = 0.5$, but if they are distributed over two dimensions in the plane of the applied field $M_r/M_s = 0.71$. The equivalent values for cubic anistropy axes are 0.82 distributed over three dimensions and 0.91 distributed over two dimensions. The measured remanence is ≈ 0.4 and is thus closest to the case for uniaxial anisotropy axes randomly distributed over three dimensions. In this case the magnetization between saturation and remanence is obtained at each field value by minimizing, over all alignments of the anisotropy axes, the intra-particle energies:

$$E_\phi = KV \sin^2(\phi - \theta) - \mu_B \cos\phi, \tag{6}$$

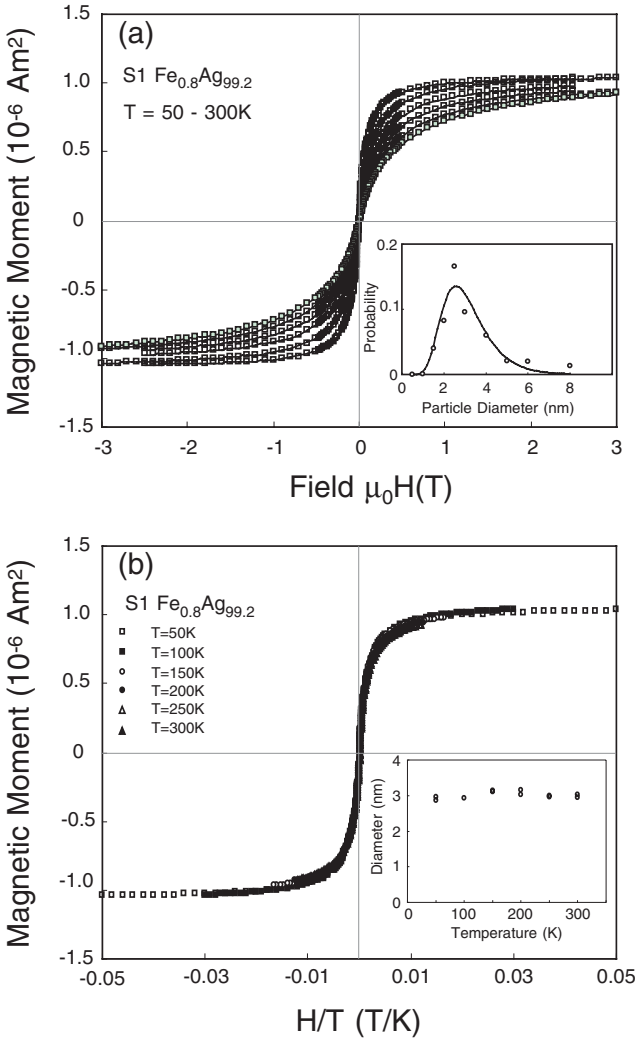

Figure 3. (a) Magnetization isotherms in the range 50–300 K of $Fe_{0.8}Ag_{99.2}$ (□) compared to fits by Langevin functions (——) with a size distribution represented by ten size bins in the range 0.5–8 nm. The inset shows the average probability of each bin for the optimum fit to curves at temperatures > 50 K (○) and the corresponding log-normal distribution (——) with $d_{max} = 2.57$ nm and $\sigma = 1.95$. (b) The same data plotted against H/T showing the scaling predicted by the Langevin functions. The inset shows the median size from the distributions as a function of temperature and demonstrates the invariance of the fitted size versus T required for an ideal superparamagnetic system.

where K is the anisotropy constant, V is the particle volume and θ and ϕ are the angles between the applied field and the anisotropy axis and particle magnetization vector respectively. The inset in figure 5(a) compares the curve calculated thus with the data and it is evident that this simple model reproduces the data accurately. So in zero field the system is a collection of static, randomly aligned cluster giant moments each pointing along the local anisotropy axis. The anisotropy constant is a parameter of the fit and is optimized at $K = 2.63 \times 10^5$ J m^{-3}, which is

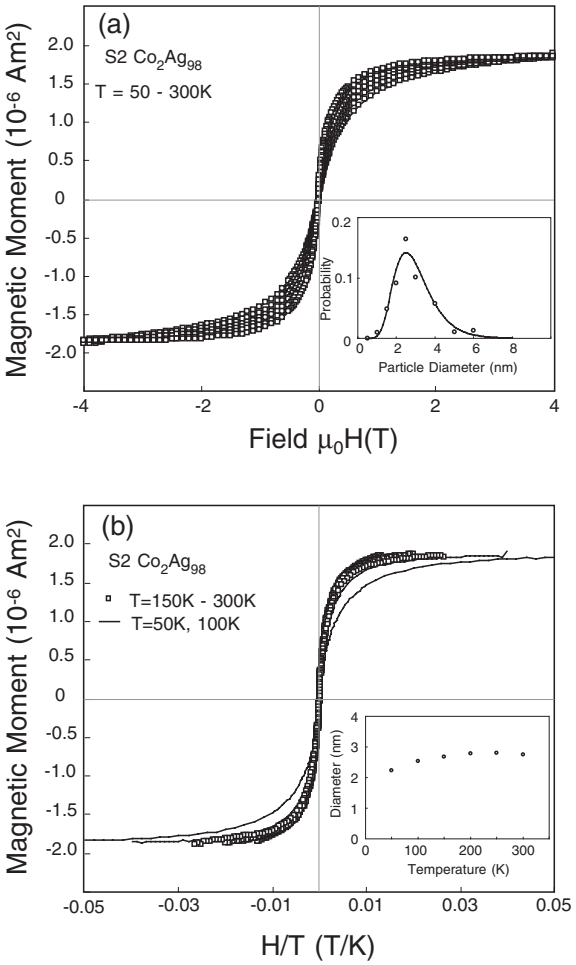

Figure 4. (a) Magnetization isotherms in the range 50–300 K of Co_2Ag_{98} (□) compared to fits by Langevin functions (——) with a size distribution represented by ten size bins in the range 0.5–8 nm. The inset shows the average probability of each bin for the optimum fit to curves at temperatures > 150 K (○) and the corresponding log-normal distribution (——) with $d_{max} = 2.45$ nm and $\sigma = 1.81$. (b) The same data plotted against H/T showing the scaling predicted by the Langevin functions for data in the range 150–300 K (□). The data at 100 and 50 K (——) show a departure from the scaling law. The inset shows the median size from the distributions as a function of temperature and demonstrates that the apparent size becomes temperature invariant (and equal to the true size) above 150 K.

in reasonable agreement with the value of $K = 2.3 \times 10^5$ J m^{-3} obtained by a previous SQUID measurement of a similar sample [32], and is about five times the bulk value.

A uniaxial anisotropy of the individual clusters is expected as it will be produced by any incomplete atomic shell. Only clusters containing magic numbers of atoms are expected to have a cubic anisotropy but even in this case it is likely to be lost due to other processes during deposition such as collision with the substrate (see below).

The blocking temperature, T_b, of a cluster with a volume V and anisotropy constant K is given by

$$T_b = \frac{KV}{k_B \ln(\tau_{\exp}/\tau_0)} \tag{7}$$

where $\tau_{\exp}$ is the measurement time ($\sim$100 s for DC magnetometry) and τ_0 is the lifetime due to the natural gyromagnetic frequency of the particles. A previous measurement [32] of Fe nanocluster embedded in Ag yielded $\tau_0 = 10^{-8}$ s so for the 3 nm Fe particles in this study with the anisotropy constant from figure 5(a) we obtain $T_b = 8.5$ K. At 2 K clusters with a diameter less than 1.4 nm, or about 5% of the distribution shown in the inset in figure 3(a), are unblocked so the remanence will be less than 0.5. This does not quantify the entire discrepancy with the data but the anisotropy constant is an average over the whole size distribution and the value is expected to increase with decreasing cluster size. This would result in more than 5% of the assembly remaining unblocked at 2 K.

Figure 5(b) shows the isotherms at 2 K for S1 with the field applied perpendicular to the surface. Ideally the magnetization in the assembly should be isotropic and superficially the curves in figures 5(a) and (b) look similar and have the same coercive field. Close inspection however reveals that the approach to saturation is slightly slower in the out-of-plane configuration as detailed in the inset. A comparison is again made with the predicted curve obtained using equation (6) and the optimum anisotropy constant is 3.52×10^5 J m^{-3}. The in-plane bias is consistent with an XMCD determination of the anisotropy of the orbital moment for deposited clusters [10]. We ascribe it to the deposition process inducing either a slight shape distortion or stress in the clusters on impact with the substrate. In addition the embedding matrix will introduce additional anisotropy terms due to magnetoelastic stress. The effect of these factors will be to introduce a coherent anisotropy over the whole film. From the difference in the anisotropy values in figure 5 ($\sim 0.9 \times 10^4$ J m^{-3}), the coherent anisotropy field ($=2\Delta K/M_s$) can be estimated to be $\sim$0.1 T.

3.4. Dilute Co cluster assemblies below the blocking temperature

In the case of the dilute Co cluster sample (S2) only the out-of-plane isotherms are available at 2 K and these are shown in figure 6. Again the remanence is slightly less than 50% and assuming the clusters are randomly oriented over three dimensions and have a uniaxial anisotropy the approach to saturation can be modelled using equation (6). This is compared to the data in the inset in figure 6 and the anisotropy constant obtained is two to three times larger than found in the Fe cluster assembly giving a blocking temperature of $\sim$20 K. The larger blocking temperature will require a higher temperature than Fe clusters to obtain superparamagnetism as observed above.

3.5. Pure cluster films

Having carefully studied the isolated particles we now turn our attention to the opposite extreme of the volume fraction range, that is, pure cluster films deposited with no matrix. As discussed in section 1 the clusters stack randomly producing a film with a granular morphology and from the analysis of the superparamagnetic isotherms from sample S1 and S2 we know the grain size distribution. Figure 7 shows the magnetization curve at 300 K of sample S3 (5 nm thick pure cluster layer with no cap) and sample S4 (20 nm thick pure Co cluster layer with no cap). In

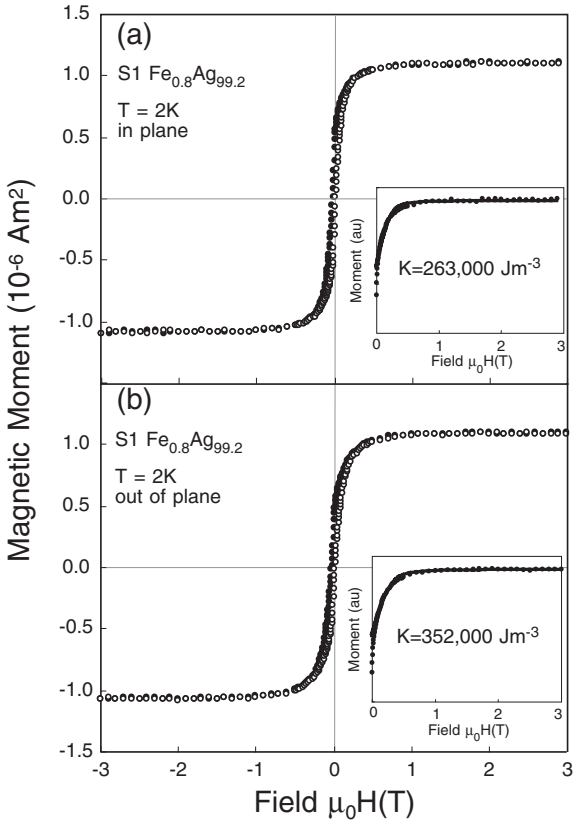

Figure 5. (a) In-plane magnetization isotherms at 2 K of sample S1 ($Fe_{0.8}Ag_{99.2}$): (●) field sweeping down, (○) field sweeping up. The inset shows the decay from saturation (●) compared to a calculation (——) assuming a random distribution of uniaxial anisotropy axes (equation (6)). The best fit anisotropy constant is displayed in the inset. (b) As (a) but with the field applied out of plane.

both cases the data are compared to the 300 K curves of the isolated clusters demonstrating the profound difference produced by strong cluster interactions. The very high initial susceptibility of the pure cluster films is characteristic of a CSSG.

We have analysed the Fe cluster film data using an RA model introduced in section 1. According to Chudnovsky [25], the approach to saturation of a system whose ground state is a CSSG is given by

$$M = M_s\left(1 - \frac{1}{32}\frac{\lambda_r^2}{\sqrt{h_{ex}}}\int_0^\infty \mathrm{d}x\, C(x)x^2 K_1\left[x\sqrt{h_{ex}}\right]\right) \tag{8}$$

in two dimensions and

$$M = M_s\left(1 - \frac{1}{30}\frac{\lambda_r^2}{\sqrt{h_{ex}}}\int_0^\infty \mathrm{d}x\, C(x)x^2 \exp\left[x\sqrt{h_{ex}}\right]\right) \tag{9}$$

in three dimensions.

In equations (8) and (9), $h_{ex} = H/H_{ex}$, $\lambda_r = H_r/H_{ex}$, K_1 is the modified Hankel function and $C(x)$ is the correlation function for the anisotropy axes with x in units of R_a. In an

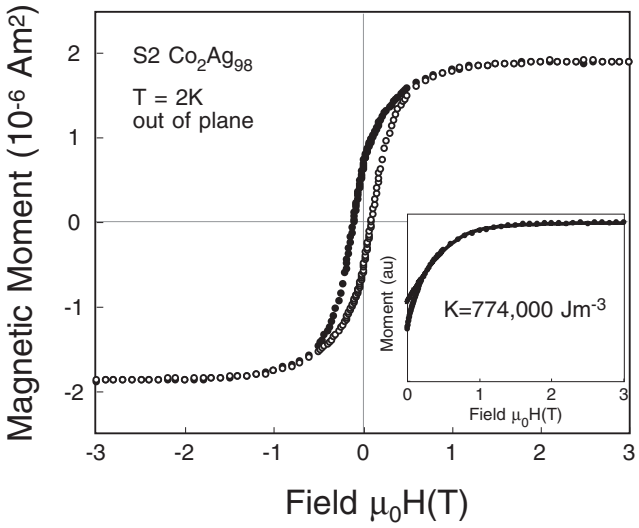

Figure 6. Out-of-plane magnetization isotherms at 2 K of sample S2 (Co_2Ag_{98}): (●) field sweeping down, (○) field sweeping up. The inset shows the decay from saturation (●) compared to a calculation (——) assuming a random distribution of uniaxial anisotropy axes (equation (6)). The best fit anisotropy constant is displayed in the inset.

amorphous metal, $C(x)$ will be a smoothly decreasing function with a characteristic decay distance of R_a. For example, $C(x) = \exp(-x^2/2)$ has been used in fits to three-dimensional spin glasses [33]. In a cluster-assembled film consisting of mono-sized particles, $C(x)$ will be a step function cutting off at $x = 1$ [34]. Here we have rounded the step function by using $C(x) = \exp(-x^8/2)$ to simulate the narrow size distribution but visually there is no discernible change to the fits if a simple step is used. We have used the two-dimensional form (equation (8)) for the approach to saturation for sample S3 as it is only two cluster layers thick whereas we have used the three-dimensional form (equation (9)) for the much thicker Co cluster film.

The only independent parameters entering equations (8) and (9) are the exchange and RA fields, H_{ex} and H_r. From the analysis of the isolated particles (figures 5 and 6) we can write the condition $K_r \leq 2.6 \times 10^5$ for Fe and $K_r \leq 7.7 \times 10^5$ for Co, i.e. from (3):

$$\begin{aligned} H_r &\leq 0.3\ \mathrm{T(Fe)} \\ H_r &\leq 0.9\ \mathrm{T(Co)}. \end{aligned} \tag{10}$$

The exchange constant, A, must be much smaller than the atomic value of $\sim 10^{-11}$ J m^{-1} giving from (4) and the median cluster diameter

$$H_{ex} \ll 1.3\ \mathrm{T}. \tag{11}$$

In addition any coherent anisotropy field, H_c must be included in the fits by replacing H with $H + H_c$ [22]. In the discussion of the isolated Fe clusters we showed that the coherent anisotropy field was ~ 0.1 T but this value includes anistropy induced by the Ag matrix. For the pure cluster films we can therefore write

$$H_c < 0.1\ \mathrm{T}. \tag{12}$$

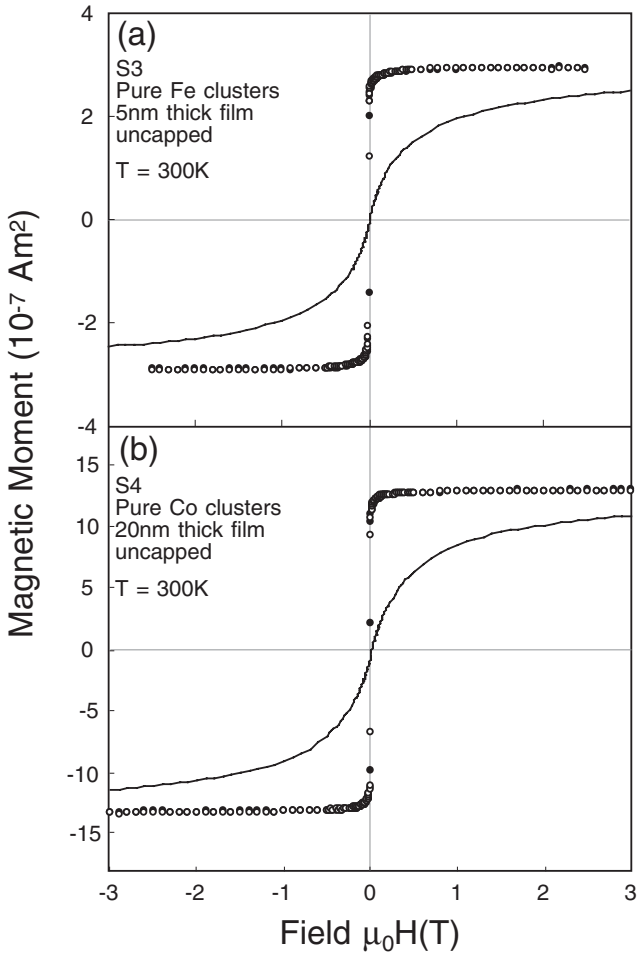

Figure 7. (a) Magnetization isotherms at 300 K of sample S3 (pure Fe clusters): (●) field sweeping down, (○) field sweeping up. The line shows the curve for the isolated clusters at 300 K. (b) As (a) but for sample S4 (pure Co clusters).

We have optimized the fits between the magnetization data, in the range between $0.85M_s$ and M_s, and the calculated curve from equations (8) and (9) as a function of the parameters H_r, H_{ex} and H_c where the variation was restricted to the ranges specified by conditions (10)–(12). The results for temperatures in the range 5–300 K are shown in figures 8(a) and (b). The first observation is the excellent agreement between the data and the RA model at all temperatures for both films reinforcing the assertion that the cluster layers form a CSSG in their ground state. It is found that in both cases the values of H_r and H_{ex} change little with temperature, which is just confirmation of the observation that the shape of the curves appears to be independent of temperature. The value of the RA, K_r, obtained from H_r and equation (3) is shown in the insets and compared to the values for the isolated clusters. For the Fe cluster film, the RA is close to the isolated cluster value whereas for the Co cluster film it is significantly smaller. The exchange fields are ≈ 0.36 and ≈ 0.6 T for the Fe and Co cluster films respectively, corresponding to an exchange constant (from equation (4)) of $A \approx 3 \times 10^{-12}$ J m^{-1} for both films, which is much less than the bulk value as required. The coherent anisotropy field remains constant with temperature and is ≈ 0.03 T for Fe and ≈ 0.01 T for Co.

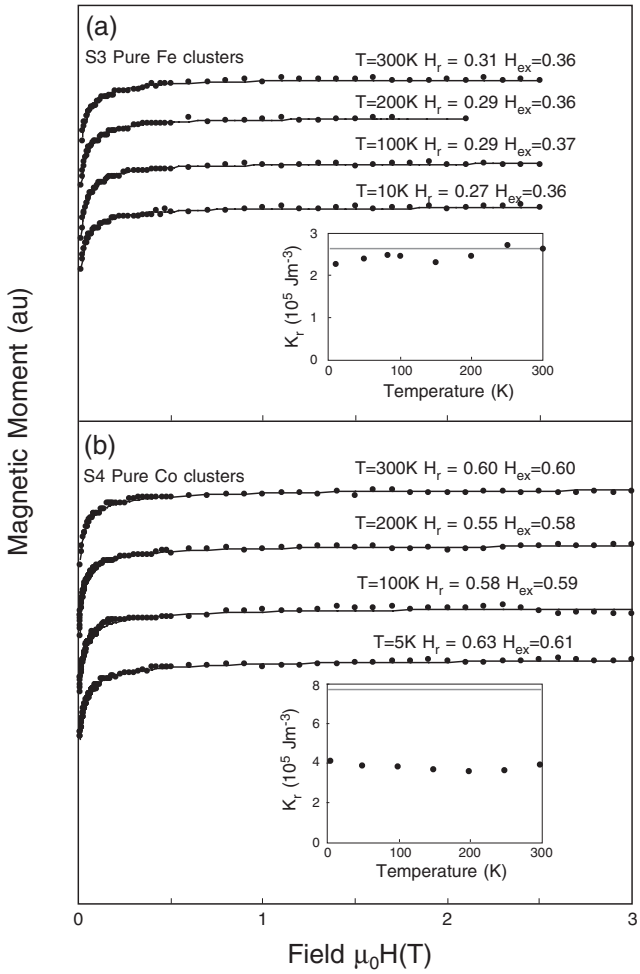

Figure 8. (a) Approach to saturation of sample S3 (5 nm thick pure Fe cluster film) for temperatures in the range 10–300 K (●) compared to a calculation using the RA model with the parameters shown (——). The inset shows the variation of the RA (evaluated from H_r and equation (3)) with temperature (●). The grey line shows the value for the isolated clusters. (b) As (a) but for sample S4 (20 nm thick pure Co cluster film).

The fits indicate that the exchange and anisotropy fields are approximately constant but according to the model [25] both should increase slightly with decreasing temperature. The fact that this is not picked up by the analysis is not surprising given the looseness of the constraints on the parameters. The behaviour is however in sharp contrast to a previous observation of a pure Fe cluster film that was sandwiched between Ag buffer and capping layers [29]. In that case the film formed a CSSG state at 300 K but a significant increase in the value of H_r with temperature was found. Below 50 K, the aniotropy was sufficiently high to produce a transition from a CSSG to a simple spin glass state in which the moment in each cluster points along the local intra-cluster anisotropy axis just as in isolated clusters below the blocking temperature. This was ascribed to mechanical stress in the film, which was deposited at room temperature so that when cooling, the higher expansion coefficient of Ag would exert a pressure on the

clusters. This is supported by the observation here, i.e. in uncapped films deposited on an organic substrate the variation of H_r with temperature is small.

4. Summary

We have studied the magnetic behaviour of films produced by depositing gas phase Fe and Co nanoclusters on surfaces in UHV. The isolated particle properties were observed by preparing samples with a very low volume fraction of the magnetic clusters in Ag matrices. The assemblies displayed ideal superparamagnetic behaviour above 50 and 150 K in the case of Fe and Co respectively. This allowed a determination of the cluster size distribution, which followed a log-normal relationship and yielded a median diameter of 3.0 nm for the Fe clusters and 2.8 nm for the Co clusters. Analysis of the low temperature magnetization curves showed that the clusters have a uniaxial anisotropy in both cases and enabled a determination of the anisotropy constants. Pure cluster films deposited with no matrix and left exposed were transferred into the VSM in UHV conditions. Both films were found to be in a CSSG state in zero field at all temperatures in the range 10–300 K.

Acknowledgments

We gratefully acknowledge support from the EC (contract G5RD-CT-2001-0047P-AMMARE) and the UK EPSRC (grant GR/N66100) for the work presented in this report.

References

[1] Stoner E C and Wohlfarth E P 1948 *Phil. Trans. R. Soc.* A **240** 599
[2] Néel L 1949 *Ann. Geophys.* **5** 99
[3] Chudnovsky E M and Friedman J R 2000 *Phys. Rev. Lett.* **85** 5206
[4] Barbara B, Chiorescu I, Giraud R, Jansen A G M and Caneschi A 2000 *J. Phys. Soc. Japan* **69** 383
[5] Barbara B, Thomas L, Lionti F, Chiorescu I and Sulpice A 1999 *J. Magn. Magn. Mater.* **200** 167
[6] Binns C 2001 *Surf. Sci. Rep.* **44** 1
[7] Billas I M L, Becker J A, Châtelain A and de Heer W A 1993 *Phys. Rev. Lett.* **71** 4067
[8] Douglass D C, Cox A J, Bucher J P and Bloomfield L A 1993 *Phys. Rev.* B **47** 12874
[9] Edmonds K W, Binns C, Baker S H, Thornton S C, Norris C, Goedkoop J B, Finazzi M and Brookes N B 1999 *Phys. Rev.* B **60** 472
[10] Edmonds K W, Binns C, Baker S H, Maher M J, Thornton S C, Tjernberg O and Brookes N B 2001 *J. Magn. Magn. Mater.* **231** 113
[11] Edmonds K W, Binns C, Baker S H, Maher M J, Thornton S C, Tjernberg O and Brookes N B 2000 *J. Magn. Magn. Mater.* **220** 25
[12] Durr H A, Dhesi S S, Dudzik E, Knabben D, van der Laan G, Goedkoop J B and Hillebrecht F U 1999 *Phys. Rev.* B **59** 701
[13] Eastham D A and Kirkman I W 2000 *J. Phys.: Condens. Matter* **12** L525
[14] Binns C, Louch S, Baker S H, Edmonds K W, Maher M J and Thornton S C 2002 *IEEE Trans. Magn.* **38** 141
[15] Parent F, Tuaillon J, Stern L B, Dupuis V, Prevel B, Perez A, Melinon P, Guiraud G, Morel R, Barthelemy A and Fert A 1997 *Phys. Rev.* B **55** 3683
[16] Yoon B, Akulin V M, Cahuzac Ph, Carlier F, de Frutos M, Masson A, Mory C, Colliex C and Bréchignac C 1999 *Surf. Sci.* **443** 76

[17] Perez A, Melinon P, Dupuis V, Jensen P, Prevel B, Tuaillon J, Bardotti L, Martet C, Treilleux M, Broyer M, Pellarin M, Vialle J L, Palpant B and Lerme J 1997 *J. Phys. D: Appl. Phys.* **30** 709
[18] Bouwen W, Kunnen E, Temst K, Thoen P, Van Bael M J, Vanhoutte F, Weidele H, Lievens P and Silverans R E 1999 *Thin Solid Films* **354** 87
[19] Eastham D A, Hamilton B and Denby P M 2002 *Nanotechnology* **13** 51
[20] Upward M D, Cotier B N, Moriarty P, Beton P H, Baker S H, Binns C and Edmonds K W 2000 *J. Vac. Sci. Technol.* B **18** 2646
[21] Chudnovsky E M 1983 *J. Magn. Magn. Mater.* **40** 21
[22] Chudnovsky E M, Saslow W M and Serota R A 1986 *Phys. Rev.* B **33** 251
[23] Saslow W M 1987 *Phys. Rev.* B **35** 3454
[24] Chudnovsky E M 1988 *J. Appl. Phys.* **64** 5770
[25] Chudnovsky E M 1995 *The Magnetism of Amorphous Metals and Alloys* ed J A Fernandez-Baca and Wai-Yim Ching (Singapore: World Scientific) ch 3
[26] Loffler J F, Braun H-B and Wagner W 2000 *Phys. Rev. Lett.* **85** 1990
[27] Thomas L, Tuaillon J, Perez J P, Dupuis V, Perez A and Barbara B 1995 *J. Magn. Magn. Mater.* **140** 437
[28] Perez J P, Dupuis V, Tuaillon J, Perez A, Paillard V, Melinon P, Treilleux M, Thomas L, Barbara B and Bouchet-Fabre B 1995 *J. Magn. Magn. Mater.* **145** 74
[29] Binns C, Maher M J, Pankhurst Q A, Kechrakos D and Trohidou K N 2002 *Phys. Rev.* B submitted
[30] Baker S H, Thornton S C, Edmonds K W, Maher M J, Norris C and Binns C 2000 *Rev. Sci. Instrum.* **71** 3178
[31] Allia P, Coisson M, Tiberto P, Vinai F, Knobel M, Novak M A and Nunes W C 2001 *Phys. Rev.* B **64** 144420
[32] Jackson T J, Binns C, Forgan E M, Morenzoni E, Niedermayer Ch, Glckler H, Hofer A, Luetkens H, Prokscha T, Riseman T M, Schatz A, Birke M, Litterst J, Schatz G and Weber H P 2000 *J. Phys.: Condens. Matter* **12** 1399
[33] Tejada J, Martinez B, Labarta A and Chudnovsky E M 1991 *Phys. Rev.* B **44** 7698
[34] Loffler J F, Meier J P, Doudin B, Ansermet J-P and Wagner W 1998 *Phys. Rev.* B **57** 2915